SECOND EDITION

ATMOSPHERIC SCIENCE FOR ENVIRONMENTAL SCIENTISTS

EDITED BY
C. N. HEWITT | ANDREA V. JACKSON

WILEY Blackwell

Atmospheric Science for Environmental Scientists

Atmospheric Science for Environmental Scientists

Edited by

C.N. Hewitt
Lancaster University
Lancaster, UK

and

Andrea V. Jackson
University of Leeds
Leeds, UK

Second Edition

WILEY Blackwell

This edition first published 2020

Edition History
Blackwell Publishing Ltd (1e, 2009)

Registered Offices
John Wiley & Sons, Inc., 111 River Street, Hoboken, NJ 07030, USA
John Wiley & Sons Ltd, The Atrium, Southern Gate, Chichester, West Sussex, PO19 8SQ, UK

Editorial Office
9600 Garsington Road, Oxford, OX4 2DQ, UK

For details of our global editorial offices, customer services, and more information about Wiley products visit us at www.wiley.com.

Wiley also publishes its books in a variety of electronic formats and by print-on-demand. Some content that appears in standard print versions of this book may not be available in other formats.

Library of Congress Cataloging-in-Publication data has been applied for

9781119515227 (paperback)

Cover Design: Wiley
Cover Image: © DANNY HU/Getty Images

Set in 9.5/12.5pt STIXTwoText by SPi Global, Pondicherry, India

10 9 8 7 6 5 4 3 2 1

Contents

List of Contributors

Janet Barlow
Department of Meteorology
University of Reading
Reading, UK

Peter Brimblecombe
School of Energy and Environment
City University of Hong Kong
Hong Kong

Martyn P. Chipperfield
School of Earth and Environment
University of Leeds
Leeds, UK

Hugh Coe
School of Earth, Atmospheric, and
Environmental Sciences
The University of Manchester
Manchester, UK

Nick Hewitt
Lancaster Environment Centre
Lancaster University
Lancaster, UK

Atul Jain
Department of Atmospheric Sciences
University of Illinois
Urbana, IL, USA

Anwar Khan
School of Chemistry
University of Bristol
Bristol, UK

John Lockwood
Formerly University of Leeds
Leeds, UK

A. Rob MacKenzie
School of Geography
Earth and Environmental Sciences
University of Birmingham
Birmingham, UK

Paul Monks
Department of Chemistry
University of Leicester
Leicester, UK

Dudley Shallcross
School of Chemistry
University of Bristol
Bristol, UK

Zongbo Shi
School of Geography, Earth and
Environmental Science
The University of Birmingham
Birmingham, UK

Natalie Theeuwes
Department of Meteorology
University of Reading
Reading, UK

Joshua Vande Hey
Department of Chemistry
University of Leicester
Leicester, UK

Richard Wayne
Physical and Theoretical Chemistry Laboratory
Department of Chemistry
University of Oxford
Oxford, UK

Paul I. Williams
School of Earth and Environmental Sciences &
National Centre for Atmospheric Science
The University of Manchester
Manchester, UK

Xiaoming Xu
Department of Atmospheric Sciences
University of Illinois
Urbana, IL, USA

Preface

When we wrote the Preface to the first edition of 'Atmospheric Science for Environmental Scientists' in 2008, we noted that never before had the teaching, learning, and researching of atmospheric science been so important. We said that society must face up to the realities of global atmospheric change, including global warming and poor air quality, and that the education of students and provision of accessible information to policy makers and the public were priorities.

More than a decade later, we can only reiterate these sentiments. In 2018, the Intergovernmental Panel on Climate Change warned that the planet will reach the crucial threshold of 1.5 °C above pre-industrial levels by as early as 2030, precipitating the risks of extreme drought, wildfires, floods, and food shortages for hundreds of millions of people. And in 2018, the World Health Organization reported that 90% of the world's population lived in places where air quality exceeded WHO guideline limits, and that more than 4 million people a year died prematurely from outdoor air pollution and a further 3 million a year from indoor air pollution.

What further warnings are needed? To help society cope with the unprecedented changes that humankind is causing to our fragile atmosphere, education must be key and policy makers must act. We hope this book helps both causes.

In putting this book together, we have drawn on some of the best experts and educators in the field of atmospheric science. We hope their knowledge and enthusiasm shines through in these chapters. Our aim is to provide succinct but detailed information on all the important aspects of atmospheric science for students of environmental science and to others who are interested in learning how the atmosphere works, how humankind is changing its composition, and what effects these changes might lead to.

We are grateful to all the experts who have contributed to this book, for all reviewers' comments, and to all our students over the years who have demonstrated the need for this volume.

October 2019

Nick Hewitt
Andrea V. Jackson

Abbreviations, Constants, and Nomenclature

ADMS	Atmospheric Dispersion Modelling System
CEE	Central and eastern Europe
CCN	cloud condensation nuclei
CFC	chlorofluorocarbons
CO_2	carbon dioxide
DMS	dimethyl sulphide
DNA	deoxyribonucleic acid
EC	elemental carbon
EM	electromagnetic
ENSO	El Niño–Southern Oscillation
EPA	Environmental Protection Agency
EU	European Union
GDP	global domestic product
GEMS/AIR	Global Environmental Monitoring System/Air
GHG	greenhouse gas
HAP	hazardous air pollutant
HCFC	hydrochlorofluorocarbons
HFC	hydrofluorocarbons
IAM	integrated assessment models
IBL	internal boundary layer
IPCC	Intergovernmental Panel on Climate Change
IR	infrared
ISAM	integrated science assessment model
ITCZ	intertropical convergence zone
LAI	leaf-area index
LW	longwave
NMHC	non-methane hydrocarbons
MAP	major air pollutant
MTBE	methyl-*tert*-butyl ether
NDVI	normalized difference vegetation index
OCS	carbonyl sulphide

OECD	Organization for Economic Cooperation and Development
PAH	polycyclic aromatic hydrocarbons
PAN	peroxyacetyl nitrate
PAR	photosynthetically active radiation
PCB	polychlorinated biphenyls
PFC	perfluorogenated carbon
PM	particulate matter
PM_{10}	particles with aerodynamic diameter less than 10 μm
ppm	parts per million
ppmv	part per million by volume (1×10^{-6})
ppbv	part per billion by volume (1×10^{-9})
pptv	part per trillion by volume (1×10^{-12})
PSS	photostationary state
SAFARI	South African Regional Science Initiative
SW	shortwave
TSP	total suspended particulates
UNEP	United Nations Environmental Programme
UV	ultraviolet
VSLS	very short-lived substances
VOC	volatile organic compounds
WHO	World Health Organization
WMO	World Meteorological Organization

Constants

c	speed of light in vacuum $2.998 \times 10^{8}\,\mathrm{m\,s^{-1}}$
g	acceleration due to gravity $9.8\,\mathrm{m\,s^{-2}}$
h	Planck's constant $6.626 \times 10^{34}\,\mathrm{J\,s}$
k	Boltzmann constant $1.381 \times 10^{34}\,\mathrm{J\,K^{-1}}$
R	gas constant $8.314\,\mathrm{J\,K^{-1}\,mol^{-1}}$ ($1.3 \times 10^{5}\,\mathrm{l\,atm\,mol^{-1}\,K^{-1}}$)
Γ_d	dry adiabatic lapse rate $9.81\,\mathrm{K\,km^{-1}}$
π	3.14159
σ	Stefan–Boltzmann constant $5.67 \times 10^{-8}\,\mathrm{W\,m^{-2}\,K^{-4}}$

Nomenclature

a	radius of a particle
A	albedo
A_s	surface albedo
B	radiative intensity of a blackbody
c_p	specific heat capacity of dry air at constant pressure ($1004\,\mathrm{J\,kg^{-1}\,K^{-1}}$)

c_v	specific heat at constant volume
C	concentration (ppm or kg m^{-3})
d	preface to variable indicating incremental quantity
d	displacement height (m)
dQ	incremental change in heat
du	incremental change in internal energy
dv	incremental change in volume
dw	incremental change in work
e	turbulent kinetic energy per unit mass (J kg^{-1})
F_B	the total flux from a black body radiator
F_s	incoming solar radiation absorbed at the surface
F	net flux
$F\uparrow$	upwelling radiative flux
$F\downarrow$	downwelling radiative flux
$\bar{F}$	net flux leaving an element or layer
F_r	total upward reflected shortwave flux
F_0	incident solar flux
G	ground heat flux (W m^{-2})
h	mean height of roughness elements (m)
h_b	depth of internal boundary layer (m)
H	sensible heat flux (W m^{-2}) or mean building height (m)
H_s	scale height
H/W	aspect ratio (-)
I	intensity of light
I_0	initial intensity of light
k	von Kármán's constant ≈ 0.4 (-)
k_a	absorption coefficient
k_e	extinction coefficient
k_s	scattering coefficient
l	distance through a gas interacting with light
L	latent heat of vaporization
L	Obukhov length (m)
L_w	Liquid water content
L_x	integral (or decorrelation) lengthscale (m)
m	refractive index
M	molar mass (of air unless otherwise specified)
n	number concentration, typically of absorbers or scatterers
p(u)	probability of windspeed u (-)
P	plant area index (-)
P, p	pressure
q	specific humidity (kg kg^{-1}, sometimes g kg^{-1}) or source emission rate (kg s^{-1})
q_*	scaling parameter for specific humidity profile (kg kg^{-1}, sometimes g kg^{-1})
r	radial distance

r_v	mass mixing ratio of water vapour
r_w	saturation mixing ratio
r_r	scattered fraction reflected upwards
R	radius of the Earth
$R(\lambda)$	action spectrum
R_n	net radiation (W m^{-2})
S	Solar constant
Sk_u	skewness statistic for downstream component of the wind (-)
Sk_w	skewness statistic for vertical component of the wind (-)
t	time (s)
t_r	scattered fraction transmitted downwards
t_t	total fraction of radiation transmitted downwards
T	temperature
T_a	transmittance of the atmosphere
T_e	effective blackbody temperature of the Earth
T_L	integral timescale (s)
T_*	scaling parameter for temperature profile (°C)
u	downstream velocity component (m s^{-1})
$\overline{u}$	mean component (m s^{-1})
u'	fluctuation around mean component (m s^{-1})
u_*	friction velocity (m s^{-1})
$\boldsymbol{U}$	velocity vector (m s^{-1})
$\overline{U}$ (z)	vertical mean wind profile (m s^{-1})
$\overline{U_h}$	mean windspeed at the top of a canopy (m s^{-1})
v	lateral velocity component (m s^{-1})
w	vertical velocity component (m s^{-1})
W	along wind building spacing (m)
x	horizontal distance in downstream direction (m)
y	horizontal distance in lateral direction (m)
z	distance, usually altitude (m)
z_h	roughness length for heat transfer (m)
z_m	height of maximum plant area index (m)
z_0	roughness length for momentum transfer (m)
z_{0r}	roughness length for rural surface (m)
z_{0u}	roughness length for urban surface (m)
z_q	roughness length for moisture transfer (m)
z^*	roughness sublayer depth (m)
z/L	Monin-Obukhov stability parameter (-)
σ	standard deviation (depends on quantity)
σ_x	downstream plume spread (m)
σ_y	lateral plume spread (m)
σ_z	vertical plume spread (m)
$\sigma(\lambda)$	absorption cross section as a function of wavelength

β upscatter or backscatter fraction
γ_s saturated adiabatic lapse rate
ΔS storage term (W m^{-2})
ΔT temperature difference between rural and urban areas (or heat island intensity) (°C)
∂ preface to variable indicating incremental quantity
θ scattering angle, or potential temperature (°C or K)
θ_0 potential temperature at the surface (°C or K)
ε emissivity
λ wavelength of light
λE latent heat flux (W m^{-2})
λ_F frontal area index (-)
ρ air density (1.2 kg m^{-3})
ρ_v density of water vapour
ρ_a density of dry air
ρ_{NIR} ratio of emitted to incident near infra-red radiation (-)
ρ_{VIS} ratio of emitted to incident visible radiation (-)
χ optical depth
τ momentum flux, or shear stress (kg m^{-1} s^{-2})
υ_e extinction coefficient (-)
ω_0 single scattering albedo
ψ_m stability function for momentum (-)

1

The Climate of the Earth

John Lockwood

Formerly University of Leeds, Leeds, United Kingdom

The causes, history, and distributions of the Earth's climates are introduced in this chapter. The combination of the distribution of incoming solar radiation across the Earth's surface and the Earth's rotation both drive and shape the observed atmosphere–ocean circulation. Important factors determining changes in climate include palaeogeography, greenhouse gas concentrations, changing orbital parameters, and varying ocean heat transport. One of the major controls of climatic changes is the greenhouse gas concentration of the atmosphere, in particular that of carbon dioxide. Before the Eocene–Oligocene boundary (≈34 Myr ago) the atmosphere–ocean circulation supported a warm atmosphere and ocean, with both poles free of permanent ice. At the Eocene–Oligocene boundary, the atmosphere–ocean circulation changed to a form similar to the present, and the first evidence of an Antarctic ice sheet is found. Falling atmospheric carbon dioxide levels probably caused this change. The waxing and waning of massive temperate latitude continental ice sheets characterize the climate of the past million years. This chapter discusses recent climate changes and evidence that they are largely driven by anthropogenic generated atmospheric carbon dioxide. In particular, recent climate changes are causing the expansion of the tropical zone and a retreat of the polar zones.

The major climate zones of the world are described, with particular attention to interannual variability, and the causes of droughts and heavy rainfalls. This includes discussions of the climatic effects of the North Atlantic Oscillation (NAO) and El Niño-Southern Oscillation (ENSO).

For more specific information on global warming and climate change science, the reader is referred to Chapter 11 in this book and to the latest reports of the Intergovernmental Panel on Climate Change, available at www.ipcc.ch.

1.1 Basic Climatology

The climate of a particular place is the average state of the atmosphere observed as the weather over a finite period (e.g. a season) for a number of different years. The so-called *climate system*, which determines the weather, is a composite system consisting of five major interactive adjoint components: the

Atmospheric Science for Environmental Scientists, Second Edition. Edited by C.N. Hewitt and Andrea V. Jackson.

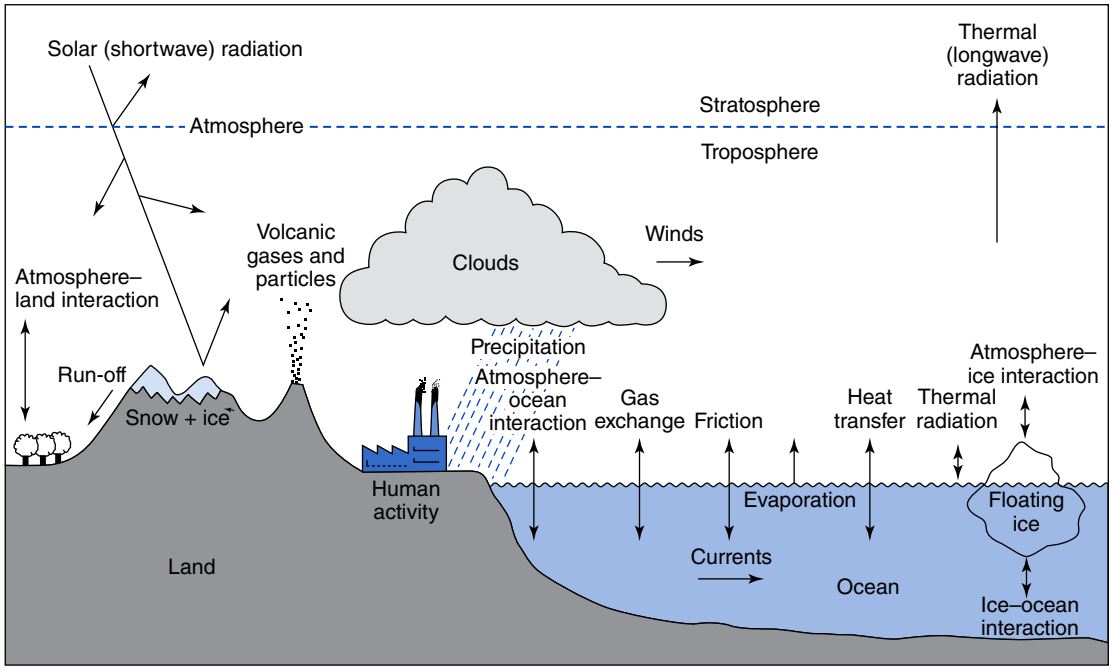

Figure 1.1 The climate system (Houghton 2005).

atmosphere, the hydrosphere, including the oceans, the cryosphere, the lithosphere, and the biosphere (Figure 1.1). All the subsystems are open and not isolated, as the atmosphere, hydrosphere, cryosphere, and biosphere act as cascading systems linked by complex feedback processes. The climate system is subject to two primary external forcings that condition its behaviour: solar radiation and the Earth's rotation. Solar radiation must be regarded as the primary forcing mechanism, as it provides almost all the energy that drives the climate system.

The distribution of climates across the Earth's surface is determined by its spherical shape, its rotation, the tilt of the Earth's axis of rotation in relation to a perpendicular line through the plane of the Earth's orbit around the Sun, the eccentricity of the Earth's orbit, the greenhouse gas content of the atmosphere, and the nature of the underlying surface. The spherical shape creates sharp north–south temperature differences, whilst the tilt is responsible for month-by-month changes in the amount of solar radiation reaching each part of the planet, and hence the variations in the length of daylight throughout the year at different latitudes and the resulting seasonal weather cycle.

The present orbit of the Earth is slightly elliptical with the Sun at one focus of the ellipse, and as a consequence the strength of the solar beam reaching the Earth varies about its mean value. At present, the Earth is nearest to the Sun in January and farthest from the Sun in July. This makes the solar beam near the Earth about 3.5% stronger than the average mean value in January, and 3.5% weaker than average in July. The gravity of the Sun, the Moon, and the other planets causes the Earth to vary its orbit around the Sun (over many thousands of years). Three different cycles are present, and when combined, produce the rather complex changes observed. These cycles affect only the seasonal and geographical

distribution of solar radiation on the Earth's surface, yearly global totals remaining constant. Surplus in one season is compensated by a deficit during the opposite one; surplus in one geographical area is compensated by simultaneous deficit in some other zone. Nevertheless, these Earth orbital variations can have a significant effect on climate and are responsible for some major long-term variations.

Firstly, there are variations in the *orbital eccentricity*. The Earth's orbit varies from almost a complete circle to a marked ellipse, when it will be nearer to the Sun at one particular season. A complete cycle from near circular through a marked ellipse back to near circular takes between 90 000 and 100 000 years. When the orbit is at its most elliptical, the intensity of the solar beam reaching the Earth must undergo a seasonal range of about 30%. Second, there is a wobble in the Earth's axis of rotation causing a phenomenon known as the *precession of the equinoxes*. That is to say, within the elliptical orbits just described, the distance between Earth and Sun varies so that the season of the closest approach to the Sun also varies. The complete cycle takes about 21 000 years. Lastly, the *tilt of the Earth's axis of rotation* relative to the plane of its orbit varies at least between 21.8° and 24.4° over a regular period of about 40 000 years. At present, it is almost 23.44° and is decreasing. The greater the tilt of the Earth's axis, the more pronounced the difference between winter and summer. Technically, these three mechanisms are known as the *Milankovitch* mechanism.

If the Earth did not rotate relative to the Sun – that is, it always kept the same side towards the Sun – the most likely atmospheric circulation would consist of rising air over an extremely hot, daylight face and sinking air over an extremely cold, night face. The diurnal cycle of heating and cooling obviously would not exist, since it depends on the Earth's rotation. Surface winds everywhere would blow from the cold night face towards the hot daylight face, whilst upper flow patterns would be the reverse of those at lower levels. Whatever the exact nature of the atmospheric flow patterns, the climatic zones on a nonrotating Earth would be totally different from anything observed today. Theoretical studies suggest that if this stationary Earth started to rotate, then as the rate of rotation increased, the atmospheric circulation patterns would be progressively modified until they resembled those observed today. In very general terms, these circulation patterns take the form of a number of meridional overturning cells in the atmosphere, with separate zones of rising air motion at low and middle latitudes, and corresponding sinking motions in subtropical and polar latitudes.

1.2 General Atmospheric Circulation

A schematic representation of the mean meridional circulation between Equator and pole is shown in Figure 1.2. A simple direct circulation cell, known as the *Hadley cell*, is clearly seen equatorward from 30° latitude (Lockwood 2003). Eastward angular momentum is transported from the equatorial latitudes to the middle latitudes by nearly horizontal eddies, 1000 km or more across, moving in the upper troposphere and lower stratosphere. This transport, together with the dynamics of the middle latitude atmosphere, leads to an accumulation of eastward momentum between 30° and 40° latitude, where a strong meandering current of air, generally known as the subtropical westerly jet stream, develops (Figure 1.3). The cores of the subtropical westerly jet streams in both hemispheres and throughout the year occur at an altitude of about 12 km. The air subsiding from the jet streams forms the belts of subtropical anticyclones at about 30° to 40° N and S (Figure 1.4). The widespread subsidence in the descending limb of the Hadley cell should be contrasted with the rising limb, where ascent is restricted to a few local areas of

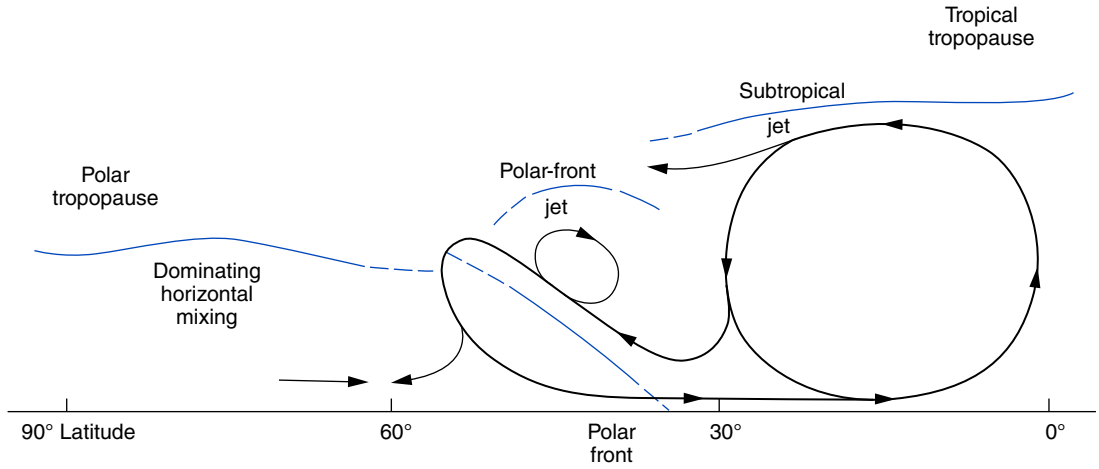

Figure 1.2 Schematic representation of the meridional circulation and associated jet-stream cores in winter. The tropical Hadley cell and middle latitude Ferrel cell are clearly visible. *Source:* from Palmen 1951.

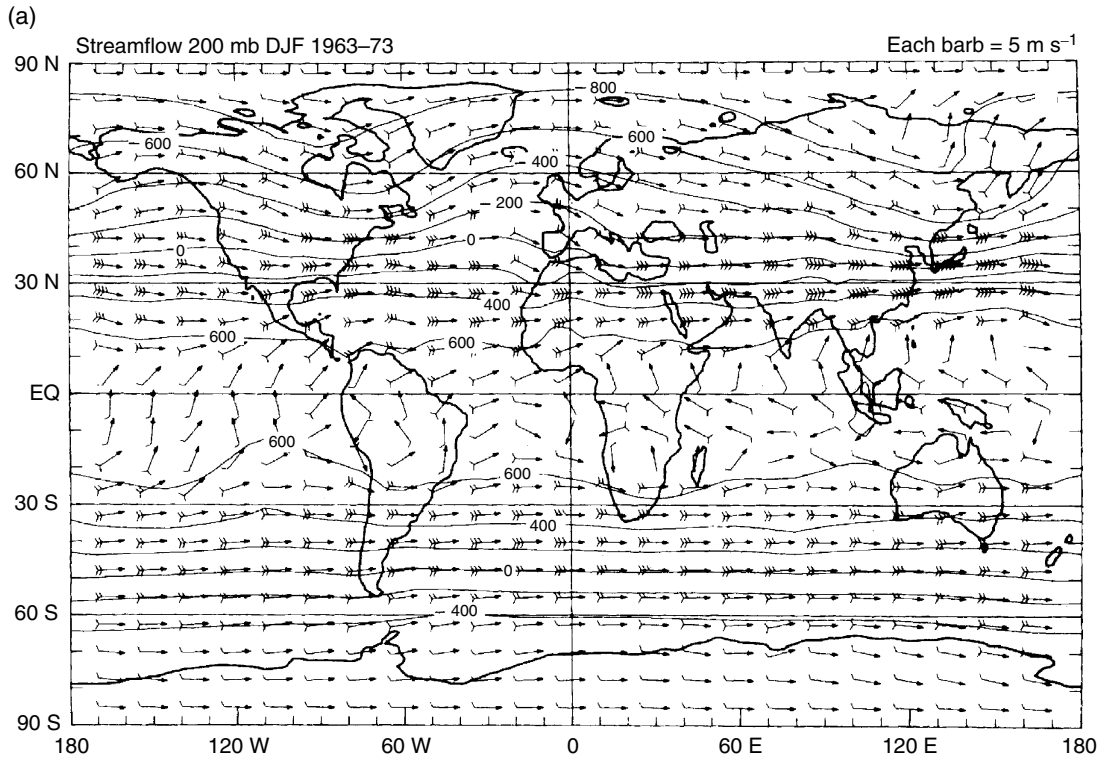

Figure 1.3 Global distribution of the mean height (1963–1973) of the 200 hPa pressure field represented as mean height minus 11 784 gpm for (a) December, January, February; (b) June, July, August. Wind speed and direction shown by arrows. Each barb on the tail of an arrow represents a wind speed of 5 m s^{-1} *Source:* from Peixoto and Oort (1992).

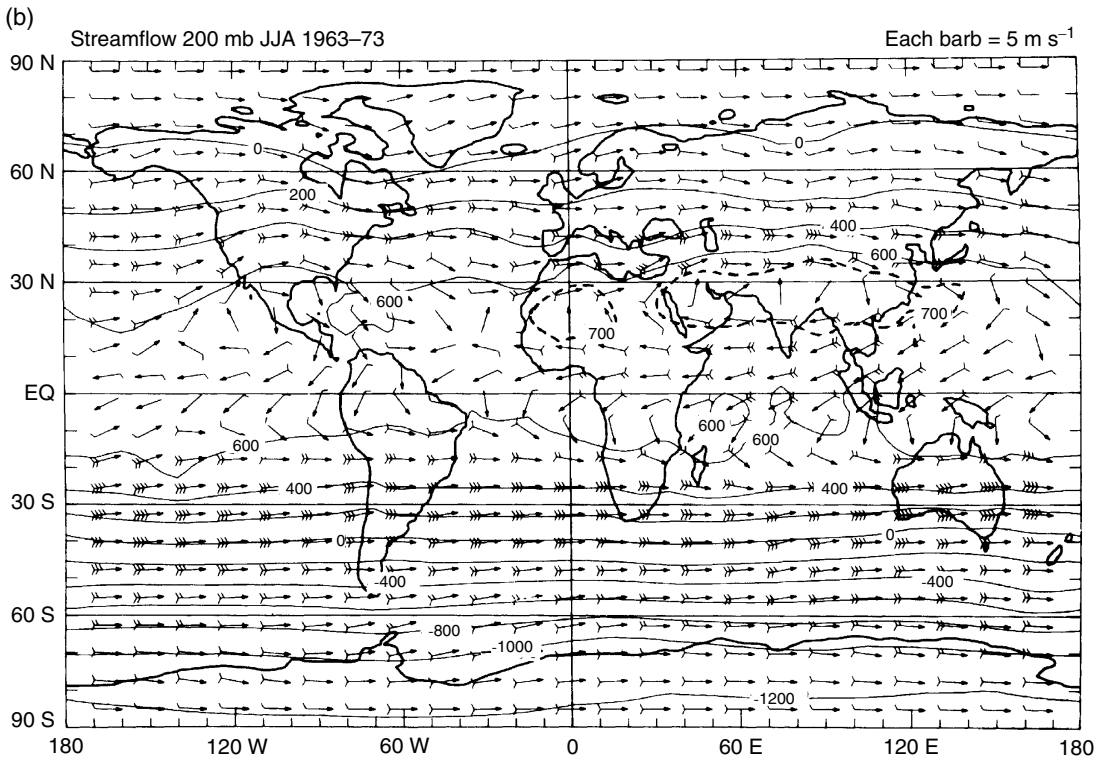

Figure 1.3 (Continued)

Figure 1.4 Mean sea-level pressure (hPa) (1963–1973) averaged for (a) December, January, February; and (b) June, July, August. *Source:* from Henderson-Sellers and Robinson (1986) and Oort (1983).

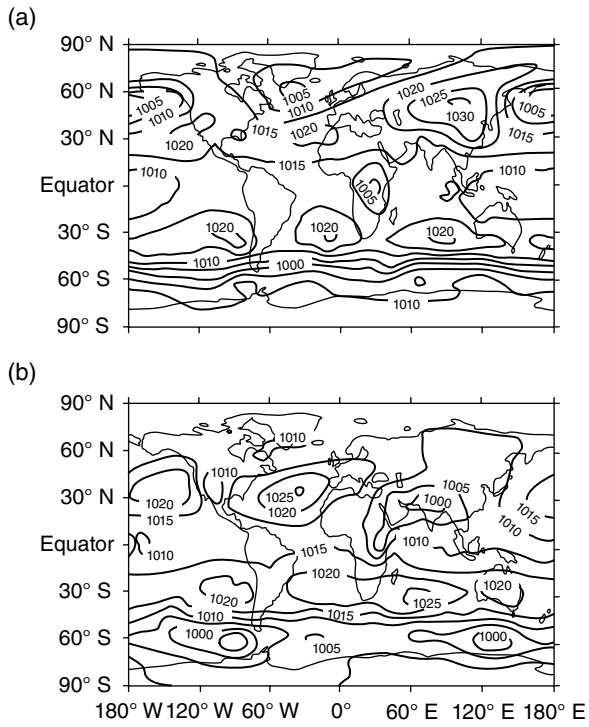

intense convection. More momentum than is necessary to maintain the subtropical jet streams against dissipation through internal friction is transported to these zones of upper strong winds. The excess is transported downwards and polewards to maintain the eastward-flowing surface winds (temperate latitude westerlies) against ground friction. The middle latitude westerly winds are part of an indirect circulation cell known as the *Ferrel cell*. The supply of eastward momentum to the Earth's surface in middle latitudes tends to speed up the Earth's rotation. Counteracting such potential speeding up of the Earth's rotation, air flows from the subtropical anticyclones towards the equatorial regions, forming the so-called *trade winds*. The trade winds, with a strong flow component directed towards the west (easterly winds), tend to retard the Earth's rotation, and in turn gain eastward momentum.

The greatest atmospheric variability occurs in middle latitudes, from approximately 40° to 70° N and S, where large areas of the Earth's surface are affected by a succession of eastward-moving cyclones (frontal depressions) and anticyclones or ridges. This is a region of strong north–south thermal gradients with vigorous *westerlies* in the upper air at about 10 km, culminating in the polar-front jet streams along the polar edges of the Ferrel cells (Figure 1.2). The zone of westerlies is permanently unstable and gives rise to a continuous stream of large-scale eddies near the surface, the cyclonic eddies moving eastward and poleward and the anticyclonic ones moving eastward and equatorward. In contrast, at about 10 km, in the upper westerlies, smooth wave-shaped patterns are the general rule. Normally, there are four or five major waves around the hemisphere, and superimposed on these are smaller waves that travel through the slowly moving train of larger waves. The major waves are often called *Rossby waves*, after Rossby who first investigated their principal properties. Compared with the Hadley cells, the middle latitude atmosphere is highly disturbed and the suggested meridional circulation shown in Figure 1.2 is largely schematic.

The extension into very high latitudes and the northward narrowing of the northern North Atlantic have consequences on the Atlantic Ocean circulation, which in turn has a series of unique effects on the climate system. This is in complete contrast to the much more benign North Pacific Ocean. Warm, saline surface water flows into the northern North Atlantic, after travelling from the Caribbean Sea, via the Gulf Stream and the North Atlantic Drift. This inflowing water, which is more saline than anywhere else in the high-latitude oceans, is finally advected to sites in the Greenland and Norwegian Seas, where extreme cooling to the atmosphere occurs and surface water sinks to the ocean depths. When cooled, water with the salinity normal in the world's oceans becomes denser, but unlike fresh water does not reach its maximum density until near its freezing point, at about −2 °C. Thus, the saltwater of the deep oceans, when cooled at the surface, goes into convective patterns, the coldest and densest portions gradually sinking from the surface to the ocean depths. Low-density surface layers in the oceans can arise either because of surface heating, or the addition of relatively fresh continental runoff or precipitation onto the ocean surface. In the cold oceans, sea-ice will form only when a layer of the ocean close to the surface has a relatively low salinity. The existence of this layer allows the temperature of the surface water to fall to freezing point, and ice to form, despite the lower levels of the ocean having a higher temperature.

1.3 Palaeoclimates

The major controls of very long-term climatic change include palaeogeography, greenhouse gas concentrations, changing orbital parameters, and varying ocean heat transport. One of the major controls on long-term climatic changes is the greenhouse gas concentration of the atmosphere and in particular that

of carbon dioxide. Atmospheric carbon dioxide concentration has varied markedly during the Earth's history. Atmospheric CO_2 concentrations are controlled by the carbon cycle, and the net effect of slight imbalances in the carbon cycle over tens to hundreds of millions of years has been to reduce atmospheric CO_2. Atmospheric CO_2 concentrations remained relatively high up to about 60 Myr ago when there was a very marked fall. Atmospheric concentrations continued to fall after about 60 Myr ago, and there is geochemical evidence that concentrations were less than 300 ppm by about 20 Myr ago.

Available evidence is that during the Mesozoic Era, temperatures ranged from 10° to 20 °C at the poles to 25–30 °C at the Equator – that is, the poles were free of permanent ice fields, and the atmosphere–ocean circulation was different in some important aspects from that observed today. Slight cooling took place at the start of the Jurassic Period and marked high-latitude warming during the first half of the Cretaceous Period. Global cooling again took place towards the end of Cretaceous time, and a long-term cooling trend commenced at the start of the Eocene Epoch, some 55 Myr ago.

The sudden, widespread glaciations of Antarctica and the associated shift towards colder temperatures at the Eocene–Oligocene boundary (approximately 34 Myr ago) is one of the most fundamental reorganizations of global climate and ocean circulation known in the geological record. Prior to the Eocene–Oligocene boundary, there is little evidence of the deep cold water in the world ocean that is so common today. Indeed, before the boundary, atmospheric, and particularly oceanic circulation conditions were probably different from those observed today. After the boundary they are probably rather similar to present-day conditions. Oceanic bottom water is formed in small regions by convective buoyancy plumes that transfer relatively dense ocean water from near the surface to the ocean depths. Deep-ocean temperatures are therefore closely related to ocean surface temperatures in key regions. The surface density and salinity is usually increased by evaporation and heat transfer to the atmosphere; therefore, virtually all deep-water formation seems to be over continental shelves in low latitudes or at high latitudes. During the Cretaceous Period and up to the end of the Eocene Epoch, the ocean bottom-waters were warm, saline, and formed in shallow subtropical marginal seas. At the Eocene–Oligocene boundary, ocean bottom-water temperatures decreased rapidly to approximately present-day levels. Deep-sea cores suggest that this change occurred within 100 000 years, which is remarkably abrupt for preglacial Tertiary times, and is considered to represent the time when large-scale freezing conditions developed at sea-level around Antarctica, forming the first significant sea-ice. At this time, cold-water plumes forming off Antarctica started to dominate ocean bottom-water formation, and together with Arctic Ocean plumes they have dominated until the present day. Thus, from early Oligocene times onwards it may be considered that world climates were in the present cold or semi-glacial state.

The initial growth of the East Antarctic Ice Sheet near the Eocene–Oligocene boundary is often attributed to the opening by continental drift of ocean gateways between Antarctica and Australia (Tasmanian Passage) and Antarctica and South America (Drake Passage), leading to the organization of the Antarctic Circumpolar current and the 'thermal isolation' of Antarctica. This notion has been challenged because although most tectonic reconstructions place the opening of the Tasmanian Passage close to the Eocene–Oligocene boundary, the Drake Passage may not have provided a significant deep-water passage until several million years later. Recent model simulations (DeConto and Pollard 2003) of the glacial inception and early growth of the East Antarctic Ice Sheet suggest that declining Cenozoic carbon dioxide first leads to the formation of small, highly dynamic ice caps on high Antarctic plateaux. At a later time, a carbon dioxide threshold is crossed, initiating various feedbacks that cause the ice caps to expand rapidly with large orbital variations, eventually coalescing into a continental-scale East Antarctic Ice sheet.

According to this simulation, the opening of the two Southern Ocean gateways plays a secondary role in this transition, relative to changing carbon dioxide concentration.

1.3.1 Quaternary Glaciations

Continental ice-sheets probably appeared in the Northern Hemisphere about 3 Myr ago, occupying lands adjacent to the North Atlantic Ocean. The time of the formation of the Greenland ice-sheet is not well known from terrestrial evidence, but the presence of glacial marine sediments in North Atlantic marine cores first appeared around 3 Myr ago. The oldest glacial moraines in Iceland are dated to approximately 2.6 Myr ago. For at least the past million years, the Earth's climate has been characterized by an alternation of glacial and interglacial episodes, marked in the Northern Hemisphere by the waxing and waning of continental ice-sheets and in both hemispheres by rising and falling temperatures (Figure 1.5). The present dominant cycle is one of about 100 kyr and is seen in the growth and decay of the continental ice-sheets. The last major glacial episode started about 110 kyr ago and finished only about 10 kyr ago. These fluctuations or cycles are found in a large number of *proxy* data records, analysis of which suggests that Antarctic air temperature, atmospheric CO_2 content, and deep-ocean temperatures are dominated by variance with a 100 kyr period and vary in phase with orbital eccentricity. In contrast, global ice volume lags changes in orbital eccentricity (Shackleton 2000). Hence, the 100-kyr ice-sheet cycle does not arise from ice-sheet dynamics; instead, it is probably the response of the global carbon cycle to changes in orbital eccentricity that generates the eccentricity signal in the climate record by causing changes in atmospheric carbon dioxide concentrations.

Proxy data records can be grouped into two climatic regimes with the transitional zone about 430 kyr ago (Figure 1.5). The earlier shows higher-frequency cycles (dominance of 40-kyr cycles), with less coherence amongst the various proxy climatic records than the later one (dominance of 100-kyr cycles). This may be due to a decrease in average atmospheric CO_2 levels over the past two million years (Brook 2005).

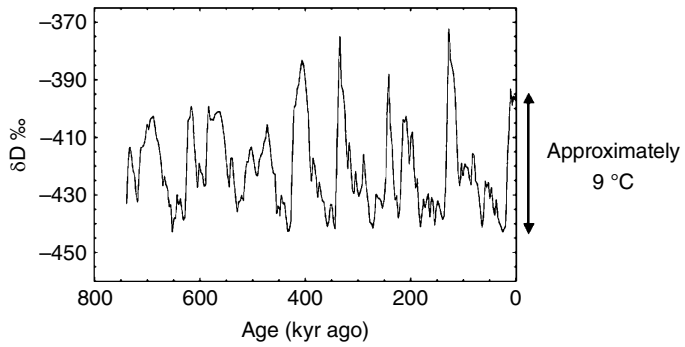

Figure 1.5 The figure shows measurements deduced from ice-cores drilled from the Antarctic ice-sheet, and analysed by the British Antarctic Survey and others as part of the European programme EPICA. The actual measurement is of the concentration of deuterium in air bubbles, and this can be related to local temperatures. The figure shows that temperature rise between the depth of the last ice age 20 000 years ago and the current interglacial is about 9 °C. *Source:* Hadley Centre for Climate Prediction and Research. From EPICA Community Members (2004).

There are differences in the amplitudes of deuterium and CO_2 oscillations before and after 430 kyr ago. The atmospheric concentration of CO_2 did not exceed 300 ppmv for the 650 000 years before the beginning (around 1750) of the industrial era. Since the Industrial Revolution, atmospheric carbon dioxide concentrations have increased by 33%. Before 430 kyr ago concentrations of CO_2 did not exceed 260 ppmv.

The transition from glacial to interglacial conditions about 430 kyr ago resembles the transition into the present interglacial period at about 10 kyr ago in terms of the magnitude of changes in temperature and greenhouse gases. As commented above, the transition 430 kyr ago also delimits the frontier between two different patterns of climate, and has been identified by recent investigations as a unique and exceptionally long interglacial. Some workers (see Brook 2005) suggest that because the orbital parameters (low eccentricity and consequently weak precessional forcing) are similar to those of the present and next tens of thousands of years, the interglacial 430 kyr ago may be the best analogue available for present and future climate without human intervention. Long interglacials with stable conditions are not, therefore, exceptional, short interglacials such as the past three are not the rule and hence cannot serve as analogues of the present Holocene interglacial.

Sudden and short-lived climate oscillations giving rise to warm events occurred many times during the generally colder conditions that prevailed during the last glacial period between 110 000 and 10 000 years ago (Lockwood 2001). They are often known as *interstadials* to distinguish them from the cold phases or *stadials*. Between 115 000 and 14 000 years ago there were 24 of these oscillations, as recognized in the Greenland ice-core records where they are called *Dansgaard–Oeschger oscillations*. These can be viewed as oscillations of the climate system about an extremely ill-defined mean state. Each oscillation contains a warm interstadial, which is linked to and followed by a cold stadial. Ice-core and ocean data suggest that the oscillations began and ended suddenly, although in general the 'jump' in climate at the start of an oscillation was followed by a more gradual decline that returned conditions to the colder 'glacial' state. Warming into each oscillation occurred over a few decades or less, and the overall duration of some of these warm phases may have been just a few decades, whereas others vary in length from a few centuries to nearly 2000 years.

Of totally different nature to Dansgaard–Oeschger oscillations are extreme and short-lived cold events, known as *Heinrich events*. These events occurred against the general background of the glacial climate and represent the climatic effects of massive surges of fresh water and icebergs from melting ice sheets into the North Atlantic, causing substantial changes in the thermohaline circulation (Lockwood 2001). Several massive ice-rafting events show up in the Greenland ice-cores as a further 3–6 °C drop in temperature from already cold glacial conditions. Many of these events have also been picked up as particularly cold and arid intervals in European and North American pollen records. The most recent Heinrich event is known as the Younger Dryas and appears as a time of glacial re-advance in Europe after the end of the main ice-age.

1.3.2 The Recent Climate Record

Extensive instrumental temperature records exist only for the period after about 1860, but recently multi-proxy data networks (e.g. Mann et al. 1999; Intergovernmental Panel on Climate Change Fifth Assessment Report, 2014) have been used to reconstruct Northern Hemisphere temperatures back to AD 1000 or earlier (Figure 1.6). These reconstructions and simulations show a long-term cooling trend in the Northern Hemisphere prior to industrialization of −0.02 °C per century, possibly related to orbital forcing, which is

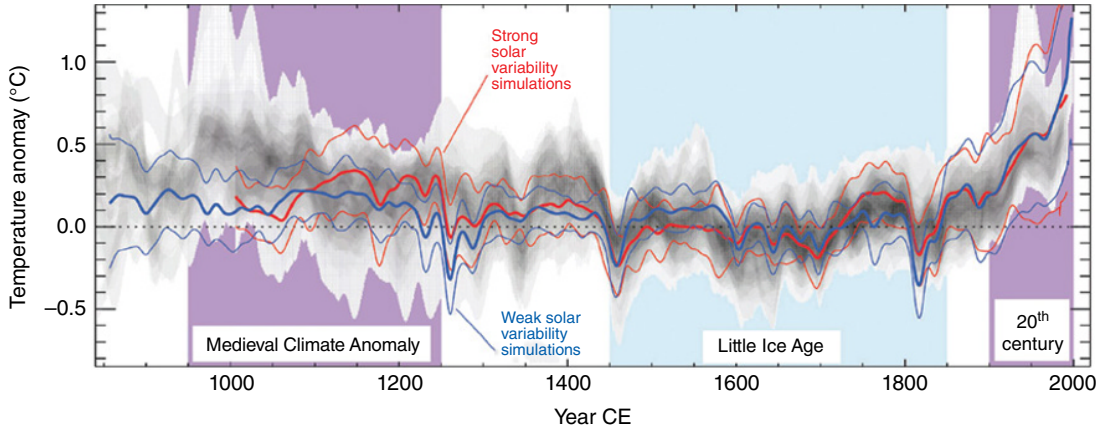

Figure 1.6 Simulated (lines) and reconstructed (grey shading) Northern Hemisphere average surface temperature changes since the Middle Ages. All data are expressed as anomalies from their 1500–1850 mean and smoothed with a 30-year filter. *Source:* data from, and more details available at, http://www.ipcc.ch/report/ar5/syr. See colour plate section for the colour representation of this figure.

thought to have driven long-term temperatures downward since the mid-Holocene at a rate within the range from −0.01 to −0.04 °C per century. The temperature reconstruction also shows that the late eleventh, twelfth and fourteenth centuries rival mean twentieth century temperature levels, whilst cooling following the fourteenth century can be viewed as the initial onset of the cold period known as the Little Ice Age. There is general agreement that the Little Ice Age came to an abrupt end around 1850, whilst studies in Switzerland indicate that overall the coldest conditions of the past 500 years were in the late seventeenth and early nineteenth centuries. The early nineteenth century was especially cold and can be considered as the 'climatic pessimism' of the past 1000 years.

Global mean surface temperature has increased dramatically during the last one hundred years or so, but not in a uniform manner (Figure 1.7). The global increase in temperature since about 1880 occurred during two sustained periods, one beginning around 1910 and another beginning in the 1970s and continuing to the present day. Best available estimates (Jones and Moberg 2003) give global temperature trends from 1910 to 1945 of 0.11 °C per decade, −0.01 °C per decade from 1946 to 1975 and 0.22 °C per decade from 1976 to 2000. In the period 2001 to 2010 warming was again ~0.11 °C per decade. Nine of the 10 warmest years observed globally since reliable observations were begun over a century and a half ago have occurred since the year 2000, and all 10 warmest years have occurred since 1998. The 20 warmest years on record have all occurred since 1995, with the five warmest years occurring since 2010. The warmest year of all (prior to 2018) was 2016.

The largest recent warming is in the winter extratropical Northern Hemisphere, with a faster rate of warming over land compared with the ocean. Using satellite-borne microwave sounding units, Qiang Fu et al. (2006) have examined atmospheric temperature trends for 1979–2005. They found that relative to the global-mean trends of the respective layers, both hemispheres have experienced enhanced tropospheric warming and stratospheric cooling in the 15–45° latitude belt. This suggests a widening of the tropical circulation zone and a poleward shift of the subtropical jet streams and their associated subtropical dry zones.